Article

Discovery Medicine 2025; 37(197): 1011–1022
https://doi.org/10.24976/Discov.Med.202537197.90

Harnessing the Power of Chlorogenic Acid: Inhibiting IL-2-Mediated Treg Upregulation to Combat Post-Traumatic Osteomyelitis

Yongpei Lin[1,*], Zhoutong Wu[2], Yan Ni[3], Ye Zhong[1], Leming Liao[1], Sai Yu[1]

[1]Department of Orthopedics, The First People's Hospital of Fuyang, 311400 Hangzhou, Zhejiang, China
[2]College of Orthopedics and Traumatology, Guangxi University of Traditional Chinese Medicine, 530011 Nanning, Guangxi, China
[3]Department of Pediatrics, Hangzhou Fuyang Hospital of Traditional Chinese Medicine, 311401 Hangzhou, Zhejiang, China
*Correspondence: linyongpei163@163.com (Yongpei Lin)
Published: 9 June 2025

Background: Chlorogenic acid (CGA) exerts immunomodulatory effects by regulating the proportion of regulatory T cells (Tregs), and T-cell dysregulation is a known feature of post-traumatic osteomyelitis (PTO). This study explored the mechanism of CGA in the treatment of PTO from the perspective of T-cell immunity.

Methods: Lymphocytes isolated from rat spleens were stimulated with interleukin (IL)-2. A PTO model was established by injecting *Staphylococcus aureus* into the tibial marrow cavity of New Zealand white rabbits. PTO rabbits were treated with either CGA by gavage or lentiviral IL-2 injection. The Treg proportion was evaluated by flow cytometry. The expression of forkhead box protein 3 (*Foxp3*), cytotoxic T lymphocyte antigen-4 (*Ctla-4*), and IL-2 was quantified by quantitative real-time polymerase chain reaction. The concentrations of tumor necrosis factor-α (TNF-α), IL-10, and IL-2 were measured using enzyme-linked immunosorbent assays. Micro-computed tomography and hematoxylin and eosin staining were performed to characterize bone destruction. The proliferation of $CD4^+$ T/$CD8^+$ T cells was evaluated by flow cytometry.

Results: IL-2 stimulation elevated the proportion of Tregs in rat splenic lymphocytes, upregulated *Foxp3*, *Ctla-4*, and IL-10 expression, and decreased TNF-α expression ($p < 0.05$). PTO rabbits exhibited significant bone destruction and inflammatory cell infiltration in bone tissue. In the peripheral blood of PTO rabbits, the Treg proportion was elevated, with increased expressions of *Foxp3*, *Ctla-4*, IL-10, and IL-2, reduced TNF-α expression, and increased proliferation of $CD4^+$ T/$CD8^+$ T cells. These changes were significantly reversed by CGA administration ($p < 0.001$). However, the reversal effects of CGA were offset by exogenous IL-2 ($p < 0.001$).

Conclusion: CGA alleviates PTO by inhibiting IL-2-mediated upregulation of Tregs.

Keywords: post-traumatic osteomyelitis; chlorogenic acid; regulatory T cells; interleukin-2; T lymphocytes

Introduction

In modern society, the rising incidence of post-traumatic osteomyelitis (PTO) parallels increasing rates of traffic accident-related injuries and geological disasters [1]. Unlike traditional osteomyelitis, PTO often presents with fractures, bone defects, and severe soft tissue damage, posing substantial therapeutic challenges [2]. Characterized by dynamic pathological changes, PTO remains a refractory condition in orthopedic surgery with high disability and recurrence rates [3]. These clinical realities underscore the urgent need for elucidating the mechanisms underlying PTO occurrence and progression and developing novel therapeutic strategies to enhance infection control, accelerate fracture healing and repair, and reduce antibiotic dependence.

There is ample evidence implicating T-cell dysregulation in PTO patients. The number of inhibitory T cells, such as regulatory T cells (Tregs), is significantly increased at the lesion sites in PTO patients [4]. Additionally, extensive T lymphocyte infiltration is observed at these sites. T lymphocytes and their secreted products play key regulatory roles in the formation and function of bone cells [5]. Tregs have also been reported to inhibit T lymphocyte immune responses in osteomyelitis [6] and to suppress T lymphocyte proliferation [7]. Therefore, Tregs may regulate the development of PTO by inhibiting T lymphocyte immune response or proliferation.

Chlorogenic acid (CGA) is a phenolic acid compound widely distributed in various plants and abundant in foods such as coffee, blueberries, apples, and vegetables [8]. As a natural antioxidant, CGA exhibits a broad range of biological activities, including antioxidative, anti-inflammatory, anticancer, and antiviral properties [9,10]. Several reports have highlighted its therapeutic potential across multiple pathological conditions. For instance, CGA attenuates epithelial-mesenchymal transition and breast cancer inva-

sion by downregulating low-density lipoprotein receptor-related protein 6 (LRP6) [11]. CGA improves cognitive deficits in sleep-deprived mice by regulating immunity function [12]. Furthermore, CGA suppresses programmed cell death ligand 1 (PD-L1) expression and enhances the antitumor immunity of programmed cell death protein 1 (PD-1) antibodies [13]. Building on this evidence, we hypothesize that CGA may regulate Tregs by mediating interleukin (IL)-2 signaling, thereby inhibiting T lymphocyte immune responses or proliferation and suppressing the development of PTO.

Materials and Methods

Animals

Male Sprague-Dawley (SD) rats (6–8 weeks old, 200–250 g, n = 5) and male New Zealand white rabbits (6–8 weeks old, 1–1.5 kg, n = 40) were obtained from Hangzhou Medical College (Hangzhou, China). Animals were housed under a natural circadian light/dark cycle, with 50% humidity and a constant temperature of 21 ± 0.5 °C.

Assessment of Lymphocyte Subsets in the Spleens of Rats

Tregs in rat spleens were detected as previously described [14]. Rats were euthanized by exsanguination following anesthesia with isoflurane (1.5% of isoflurane/air (v/v)) by using an isoflurane vaporizer (Table Top Anesthesia Machine Model V-1, Vet Equip, Pleasanton, CA, USA). Rat spleens were collected, and the tissue was mechanically ground. The suspension was filtered through a 400-mesh filter and subjected to lymphocyte isolation using a lymphocyte separation solution (40504ES60, YEASEN, Shanghai, China). Isolated lymphocytes were cultured in Roswell Park Memorial Institute (RPMI) 1640 medium (R101, YaJi Biological, Shanghai, China) supplemented with 20% fetal bovine serum (FBS, 02324, YaJi Biological, Shanghai, China). According to the experimental design, IL-2 (HY-P70718, Medchemexpress, Shanghai, China) was added to the culture medium for varying treatment time points (0, 3, 6, 12, and 24 h). Samples were stained with phycoerythrin (PE)-labeled anti-CD25 antibody (202105, Biolegend, San Diego, CA, USA) and fluorescein isothiocyanate (FITC)-labeled anti-CD4 antibody (201505, Biolegend, San Diego, CA, USA). Following a 30-minute incubation, Treg proportions were analyzed using a flow cytometer (CytoFlex, Beckman, Brea, CA, USA).

Establishment of the PTO Model

The PTO model was established as described previously [15,16]. New Zealand white rabbits were acclimated for 1 week, then anesthetized with isoflurane (2% of isoflurane/air (v/v)) by using an isoflurane vaporizer (Table Top Anesthesia Machine Model V-1, Vet Equip, Pleasanton, CA, USA) and fixed on the operating table. Hair was removed from the proximal right tibia of the rabbits. After iodophor disinfection, a 1 cm longitudinal incision was made on the medial side of the right tibia below the patella. After the blunt separation of soft tissue, the end of the tibia was exposed. A 1 mm drill was used to access the medullary cavity, from which 0.5 mL of bone marrow was extracted. Subsequently, 0.3 mL of 5% sodium morrhuate (Shanghai Xinyi Jinzhu Drug Co., Ltd., Shanghai, China) was injected into the cavity. After 5 min, 0.1 mL of *Staphylococcus aureus (S. aureus)* suspension (1×10^8 Colony-Forming Units (CFU)/mL, B81854, MingzhouBio, Ningbo, China) was injected into the cavity, and the opening was sealed with bone wax (19-5025, HuayonBio, Shenzhen, China). The wound was then sutured. After 28 days, 35 model rabbits were obtained. Successful modeling was evaluated by referring to the criteria proposed by Worlock *et al.* [16]: (1) X-ray findings of bone destruction, osteophyte formation, and soft tissue abscess; (2) Histological evidence of abscess formation, necrotic bone, subperiosteal new bone formation, and multinucleated giant cell infiltration; (3) Positive bacterial culture for *Staphylococcus aureus*. The modeling was considered successful if two of the above criteria were met.

Preparation of Lentivirus

An *IL-2* lentiviral vector (pLV[Exp]-CMV > rbIL2[NM_001163180.1], rabbit) and a negative control vector (NC, pLV[Exp]-CMV > ORF_Stuffer) were provided by VectorBuilder (Guangzhou, China). These vectors were transfected into HEK293 cells (YS809C, YaJi Biological, Shanghai, China) using a transfection reagent (C0533, Beyotime, Shanghai, China). Supernatants were collected 48 h post-transfection. HEK293 cells underwent short tandem repeat (STR) analysis and were tested for mycoplasma contamination. The *IL-2* lentiviral vector used for intrathecal injection had a titer of 10^9–10^{10} IU/mL.

Experimental Groups

The rabbit experiments were divided into two parts. The first part included four groups (n = 5 in each group): control group (normal culture), model group (*S. aureus* injection into the tibial marrow cavity of New Zealand white rabbits), model + vehicle group (model rabbits were given 20 mL of normal saline daily by gavage for 4 weeks), and model + CGA group (model rabbits were given 800 mg/kg CGA [50% purity, provided by Chengdu Hengfeng Tiancheng Technology, Chengdu, China] by gavage daily for 4 weeks) [17]. The CGA supplementation level was based on our previous study [18].

The second part comprised four groups (n = 5 in each group): model group (*S. aureus* was injected into the tibial marrow cavity of New Zealand white rabbits), model + CGA group (model rabbits were given 800 mg/kg CGA daily by gavage for 4 weeks), model + CGA + negative control (NC) group, and model + CGA + IL-2 group. In the lat-

ter two groups, rabbits were injected via the tail with either IL-2 expressing lentivirus (10^9–10^{10} IU/mL) or lentivirus-NC 24 h [19] before *S. aureus* inoculation, followed by CGA gavage (800 mg/kg) daily for 4 weeks. At day 28, the peripheral blood (5 mL) was collected from the central ear artery and transferred into 5 mL ethylenediaminetetraacetic acid (EDTA) anticoagulant tubes for subsequent experiments. Rabbits were then anesthetized with sodium pentobarbital (80 mg/kg, P3761, Sigma-Aldrich, St. Louis, MO, USA) and euthanized by exsanguination. A transverse incision was made in the femoral triangle to expose and sever the femoral artery and vein, allowing complete blood drainage. The experimental workflow is shown in **Supplementary Fig. 1**.

Micro-Computed Tomography (Micro-CT) Analysis

The tibia was analyzed using micro-CT scanning (MCT-III, Zhongke Kaisheng, Guangzhou, China). The scanning parameters were set according to previously described methods [15].

Histological Analysis

A cross-section of the mid-tibia was collected from each rabbit after being put to death, fixed in 4% paraformaldehyde solution (P0099-3L, Beyotime, Shanghai, China), decalcified, and embedded in paraffin. The paraffin-embedded tissue was sectioned into 5-µm slices and sequentially immersed in xylene and graded ethanol solutions to facilitate dewaxing and rehydration. The sections were then soaked in hematoxylin solution, differentiation solution, and stained with hematoxylin and eosin (HE), following the protocol provided with the HE staining kit (PH0516, Phygene, Fuzhou, China). After staining, the sections were dehydrated, cleared, sealed, and examined under a microscope (N300M, Yongxin, Ningbo, China).

Quantitative Real-Time Polymerase Chain Reaction (qRT-PCR)

Total RNA from $CD25^+CD4^+$ Tregs or peripheral blood was extracted using an RNA extraction kit (NP06011, NucleoTech, Beijing, China) and reverse transcribed into cDNA using a reverse transcription kit (NN01012, NucleoTech, Beijing, China). qRT-PCR was conducted using a SYBR Green kit (NL02021, NucleoTech, Beijing, China). The $2^{-\Delta\Delta CT}$ method was used to normalize the expression levels of target genes to glyceraldehyde-3-phosphate dehydrogenase (*GAPDH*). The primer sequences used for qRT-PCR are listed in Table 1.

Table 1. Primer sequences used in this study.

Gene	Primer sequence (5′ → 3′)
Foxp3 (Rat)	
Forward	GGCAGAGGACACTCAATGAAAT
Reverse	TCTCCACTCGCACAAAGCAC
Ctla-4 (Rat)	
Forward	AAGCCATACAAGTGACCCAACCTTC
Reverse	CGGACCTCATCAGTGTTGTGTGAAG
Gapdh (Rat)	
Forward	ATGCCATCACTGCCACTCA
Reverse	CCTGCTTCACCACCTTCTTG
Foxp3 (Rabbit)	
Forward	CAGTGCCCCTAGTCATGGTG
Reverse	GAACAGGCTGTCTGAGGCTT
Ctla-4 (Rabbit)	
Forward	CCTTGCAGCCATTAGTTCGG
Reverse	AATTGCTTTTCACACTCGGGC
IL-2 (Rabbit)	
Forward	TGCCCAAGAAGGTCACAGAA
Reverse	GAGCCCCTAGGGCTTACAAA
Gapdh (Rabbit)	
Forward	AGTATGATTCCACCCACGGC
Reverse	GATGGCCTTCCCGTTGATGA

Abbreviations: *Gapdh*, glyceraldehyde-3-phosphate dehydrogenase; *Foxp3*, forkhead box protein 3; *Ctla-4*, cytotoxic T lymphocyte antigen-4; *IL-2*, interleukin-2.

Enzyme-Linked Immunosorbent Assay (ELISA)

The concentrations of tumor necrosis factor-α (TNF-α) and IL-10 in the supernatants of $CD25^+CD4^+$ Tregs and peripheral blood were determined using corresponding ELISA kits (ml002859/ml002813/ml028087/ml027828, mlbio, Shanghai, China). Briefly, blood samples were centrifuged at 1000 g for 10 min. Standards or samples and biotinylated antibodies were added to the appropriate wells and incubated at room temperature for 45 min. After washing, the horseradish Peroxidase (HRP) enzyme conjugate working solution was added to each well and incubated for an additional 30 min. The substrate solution was then added and cultured for 15 min at room temperature. The reaction was stopped with a termination solution, and absorbance was measured at 450 nm using a microplate reader (CMax Plus, Molecular Devices, Shanghai, China). A standard curve (with concentration on the x-axis and Optical Density (OD) values on the y-axis) was generated, and the corresponding sample concentrations were determined based on their OD values.

Flow Cytometry

To determine the proportion of Tregs in rabbit peripheral blood, anti-CD-4 antibody (ab194998, Abcam, Cambridge, UK), anti-CD25 antibody (551779, BD, San Jose, CA, USA), and the corresponding secondary antibodies (ab150113 and ab150115, Abcam, Cambridge, UK) were used. Flow cytometry was then performed to analyze the results.

$CD4^+$/$CD8^+$ T lymphocyte proliferation was assessed as previously described [20]. Peripheral blood mononuclear cells (PBMCs) were isolated from rabbit peripheral blood using lymphocyte separation solution

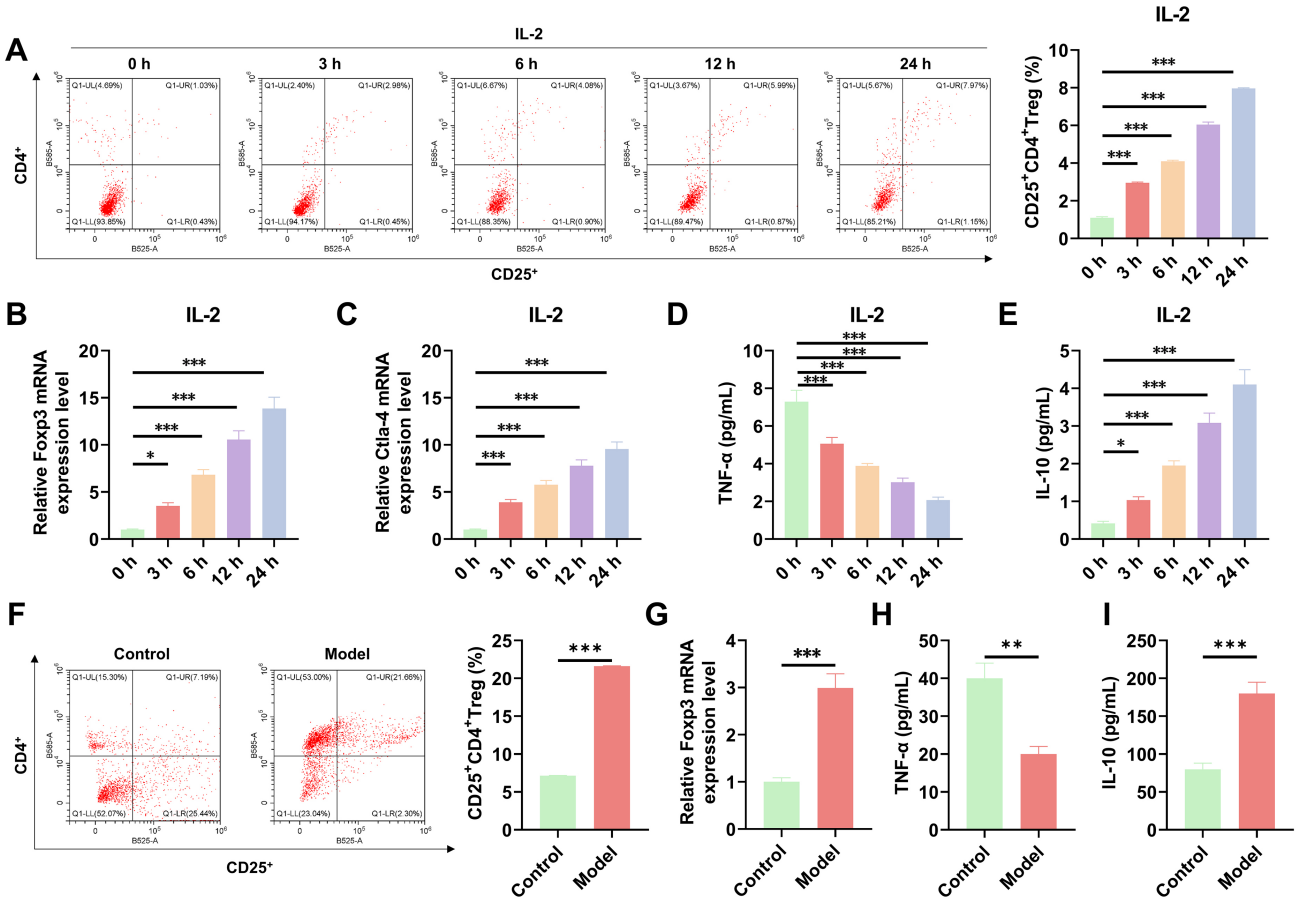

Fig. 1. Upregulation of CD25$^+$CD4$^+$ Treg in the PTO model. (A–E) Lymphocytes isolated from rat spleens were cultured with IL-2 (500 U/mL) for the indicated time points (0, 3, 6, 12, and 24 h). (A) The proportion of CD25$^+$CD4$^+$ Treg was detected by flow cytometry. (B,C) *Foxp3* and *Ctla-4* mRNA expression levels were determined by qRT-PCR, with *Gapdh* as an internal control. (D,E) TNF-α and IL-10 concentrations in the cell culture supernatants were measured by ELISA. (F–I) A PTO animal model was established by injecting *Staphylococcus aureus* into the tibial marrow cavity of New Zealand white rabbits, after which peripheral blood was collected. (F) The proportion of CD25$^+$CD4$^+$ Treg was measured by flow cytometry. (G) *Foxp3* expression was quantified by qRT-PCR. Gapdh served as an internal control. (H,I) TNF-α and IL-10 concentrations in peripheral blood were examined by ELISA. All assays were performed in triplicate and/or repeated in at least three independent experiments. *$p < 0.05$, **$p < 0.01$, ***$p < 0.001$. Abbreviations: IL-2, interleukin-2; qRT-PCR, quantitative real-time polymerase chain reaction; Gapdh, glyceraldehyde-3-phosphate dehydrogenase; ELISA, enzyme-linked immunosorbent assay; *Foxp3*, forkhead box protein 3; *Ctla*-4, cytotoxic T lymphocyte antigen-4; Treg, regulatory T cell; TNF-α, tumor necrosis factor-α; PTO, post-traumatic osteomyelitis.

(40504ES60, YEASEN, Shanghai, China) and then inoculated into 96-well plates. An additional mixture of anti-CD3 and anti-CD28 antibodies (MA5-14524, ThermoFisher, Waltham, MA, USA) was added to the 96-well plates to stimulate the cells, followed by 72 h of incubation. Subsequently, 10 µM Brdu (6813, Cell signaling technology, Danvers, MA, USA) was added to the plates and incubated for an additional 4 h. Cells were stained with PE labeled anti-BrdU antibody (364115, Biolegend, San Diego, CA, USA) and FITC-labeled anti-rabbit CD4/CD8 antibody (ab194998/ab41323, Abcam, Cambridge, UK) and analyzed by flow cytometry.

Statistical Analysis

Statistical analysis was performed using GraphPad Prism 8.0 (GraphPad Software, San Diego, CA, USA). The measurement data were expressed as mean ± standard deviation. Differences between the two groups were evaluated by independent sample *t*-test, while one-way analysis of variance (ANOVA) was used for comparisons among multiple groups. *Tukey's* test was exploited for post hoc multiple comparisons. Differences were considered statistically significant at $p < 0.05$.

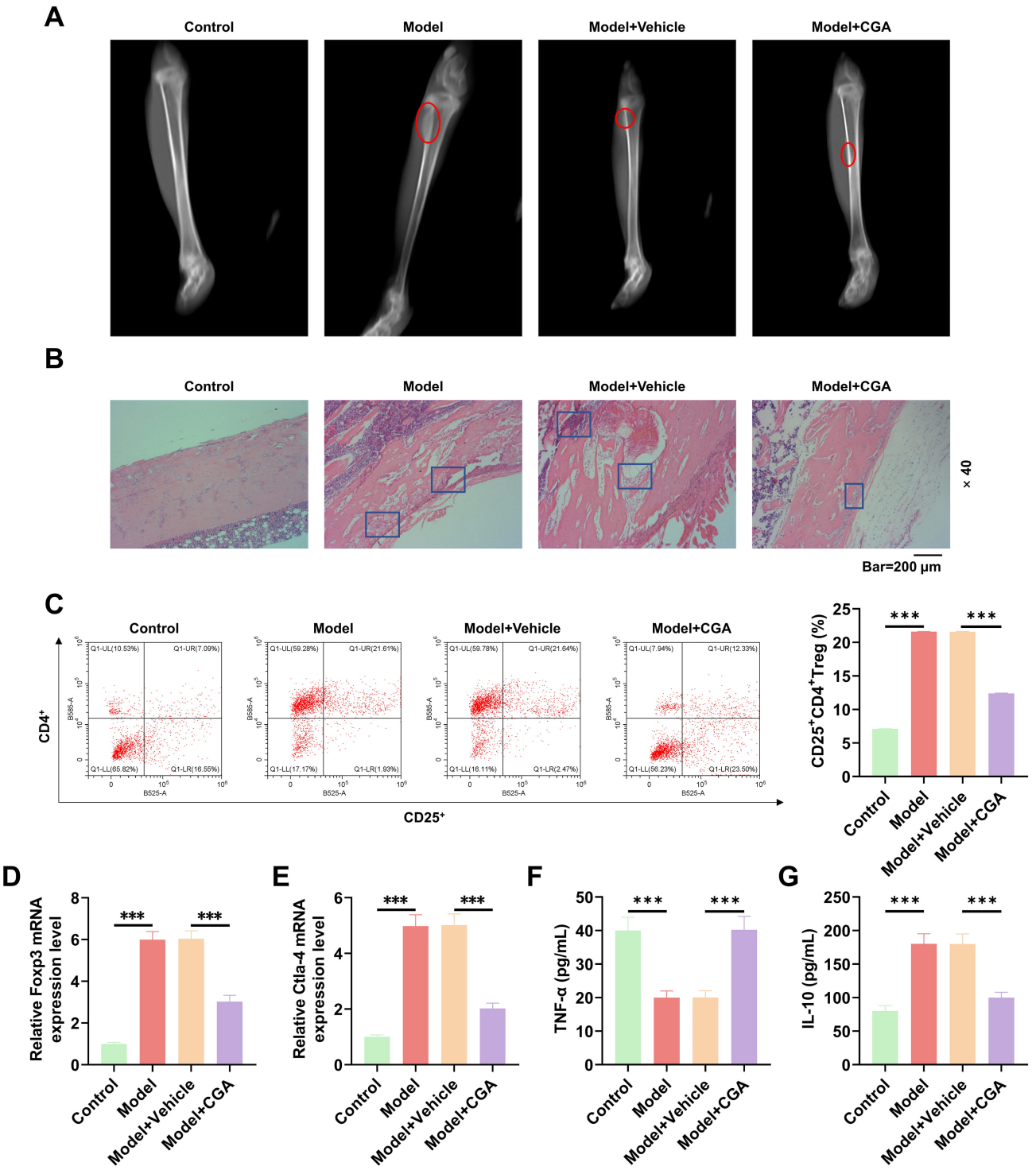

Fig. 2. Therapeutic effects of CGA on the rabbit model of PTO. New Zealand white rabbits were divided into four groups (n = 5/each group): control group (normal culture), model group (*Staphylococcus aureus* injected into the tibial marrow cavity), model + vehicle group (model rabbits treated with normal saline for 4 weeks), and model + CGA group (model rabbits treated with CGA for 4 weeks). (A) Micro-CT images of tibial defects (red circles indicate hyperosteogeny and inflammation). (B) Histological alterations were evaluated by HE staining (40× magnification, scale bar = 200 μm); blue boxes indicate osteoporosis, severe cortical bone destruction, fibrous tissue hyperplasia, and inflammatory cell infiltration. (C) The proportion of $CD25^+CD4^+$ Treg cells was analyzed by flow cytometry. (D,E) *Foxp3* and *Ctla-4* expression levels were determined by qRT-PCR with *Gapdh* as an internal control. (F,G) TNF-α and IL-10 levels in peripheral blood were quantified by ELISA. All assays were performed in triplicate and/or repeated in at least three independent experiments. ***p <0.001. Abbreviations: Micro-CT, micro-computed tomography; CGA, chlorogenic acid; HE, hematoxylin and eosin.

Results

IL-2 Stimulation Elevated the Proportion of Tregs in Rat Spleen Lymphocytes

Stimulation of rat spleen lymphocytes (n = 5) with IL-2 resulted in a significant time-dependent increase in the proportion of $CD25^+CD4^+$Treg (Fig. 1A, $p < 0.001$). This was accompanied by elevated expressions of forkhead box protein 3 (*Foxp3*) and cytotoxic T lymphocyte antigen-4 (*Ctla-4*) (Fig. 1B,C, $p < 0.05$), which are markers of Treg cells and T cell activation, respectively. Additionally, prolonged IL-2 stimulation gradually decreased TNF-α levels in the cell-conditioned medium, while IL-10 levels increased progressively (Fig. 1D,E, $p < 0.05$).

CGA Alleviated PTO Symptoms in Rabbits by Reducing Treg Proportions in Peripheral Blood

A PTO model was established in New Zealand white rabbits. In model rabbits, the proportion of $CD25^+CD4^+$ Treg (Fig. 1F, $p < 0.001$) and Foxp3 expression (Fig. 1G, $p < 0.001$) in peripheral blood were significantly elevated accompanied by a marked decrease in TNF-α levels (Fig. 1H, $p < 0.01$) and an increase in IL-10 levels (Fig. 1I, $p < 0.001$). Moreover, micro-CT imaging of the model rabbits showed osteomyelitis, characterized by bone destruction and periosteal bone formation (Fig. 2A). HE staining further revealed the presence of a large number of inflammatory cells in the bone tissue and damaged bone tissue (Fig. 2B). Notably, CGA treatment alleviated these pathological changes (Fig. 2A,B), as evidenced by a decreased proportion of $CD25^+CD4^+$ Treg (Fig. 2C, $p < 0.001$), downregulation of *Foxp3* and *Ctla-4* in peripheral blood (Fig. 2D,E, $p < 0.001$), upregulation of TNF-α (Fig. 2F, $p < 0.001$), and downregulation of IL-10 (Fig. 2G, $p < 0.001$).

CGA Inhibited CD4+/CD8$^+$T Cell Proliferation and IL-2 Expression in Peripheral Blood Cells of Model Rabbits

Compared to the control group, the model group showed higher Brdu expression in $CD4^+/CD8^+$ T cells, indicating increased proliferation of these cells (Fig. 3A). Following CGA treatment, $CD4^+/CD8^+$ T cell proliferation was significantly suppressed in the model group (Fig. 3A–C). Moreover, the model rabbits exhibited increased IL-2 protein and mRNA levels in peripheral blood, a trend that was inhibited by CGA treatment (Fig. 3D,E, $p < 0.001$).

IL-2 Reversed the Therapeutic Effects of CGA in the PTO Rabbit Model

To investigate whether the therapeutic effects of CGA on model rabbits were associated with IL-2 inhibition, we administered lentivirus-mediated IL-2 overexpression. In CGA-treated rabbits, the addition of IL-2 exacerbated bone destruction and inflammatory cell infiltration in bone tissue (Fig. 4A,B). Additionally, it further increased the proportion of $CD25^+CD4^+$ Treg in peripheral blood (Fig. 4C, $p < 0.001$) and upregulated *Foxp3*, *Ctla-4*, and IL-10 expression while suppressing TNF-α expression (Fig. 4D–G, $p < 0.001$). Moreover, the CGA-induced inhibition of $CD4^+/CD8^+$ T cells proliferation and downregulation of IL-2 expression were reversed by IL-2 overexpression (Fig. 5A–E, $p < 0.001$).

Discussion

PTO is a complex disease with a high recurrence rate, posing significant risks, such as amputation and life-threatening complications, placing a heavy burden on patients and their families. Although the current study did not directly investigate the role of CGA in treating PTO, our findings shed light on its potential therapeutic mechanisms from the perspective of Treg regulation, given the known association between PTO and immunosuppression.

The previous study has indicated that the survival and maintenance of the inhibitory phenotype of Tregs are associated with IL-2 [21]. We treated spleen lymphocytes of rats with IL-2 and observed a significant increase in the proportion of Tregs, and elevated levels of Foxp3 (a specific expression marker of Treg on the cell surface), Ctla-4, and IL-10, which are cytokines with immunosuppressive roles in Tregs. Moreover, IL-2 stimulation led to a decrease in TNF-α, a key inflammatory mediator. In previous research, IL-2/Interleukin-2 Receptor (IL-2R) signaling alone was shown to fine-tune TNF-α concentration, while Tregs treated with IL-2/IL-2R antibody complexes could further reduce TNF-α levels [22]. It has been reported that Tregs can produce TNF-α under certain inflammatory conditions, and TNF-α, in turn, can attenuate the immunosuppressive function of Tregs [23]. Therefore, our findings suggest that IL-2 may decrease TNF-α by enhancing the immunosuppressive function of Tregs, thereby interrupting the Treg-TNF-α-Treg feedback loop.

The PTO rabbit model was established using *Staphylococcus aureus* due to its role as a primary pathogen in osteomyelitis [24,25], and we observed an increase in peripheral blood Tregs and bone tissue destruction, aligning with a previous report [26]. Treg cells are usually upregulated in inflammatory conditions due to their immunosuppressive properties, which help regulate inflammation and immune responses [27,28]. Additionally, we observed increased proliferation of $CD4^+/CD8^+$ T cells in PTO rabbits. This finding aligns with the previous study that has reported extensive T lymphocyte infiltration at infection sites in PTO patients and expansion of $CD8^+$ T cells in peripheral blood [29]. $CD8^+$ T cells are involved in the elimination of intracellular bacteria and can identify and kill other cells infected with *S. aureus* [30]. $CD4^+$ T cells mediate the activity of other immune cells to indirectly combat infections [31]. However, abnormal proliferation of T lymphocytes leads to persistent bone destruction. Specifically,

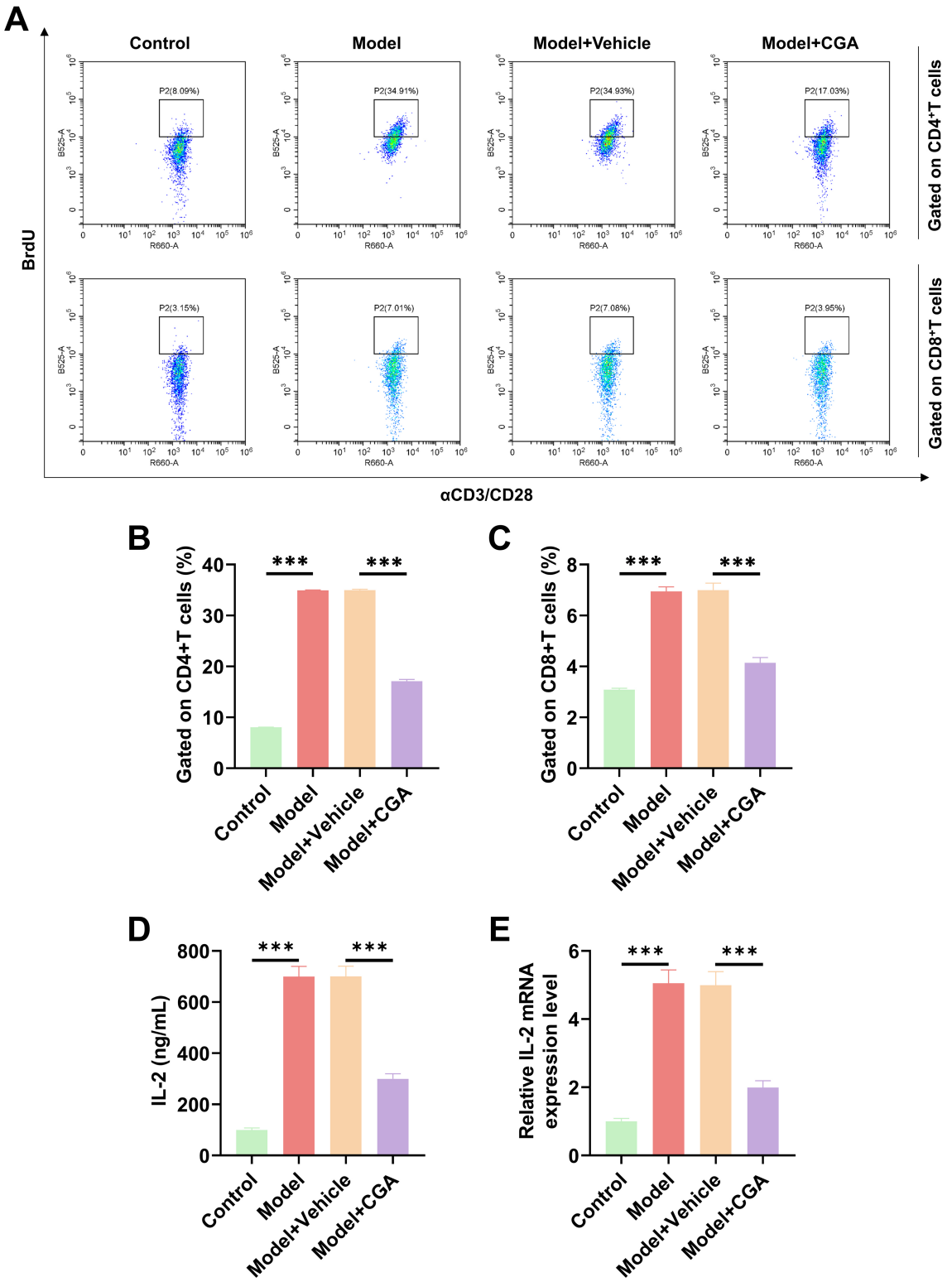

Fig. 3. Effects of CGA on CD4$^+$ or CD8$^+$T lymphocyte proliferation and IL-2 expression in PTO rabbits. New Zealand white rabbits were divided into four groups (n = 5/each group): control group (normal culture), model group (*Staphylococcus aureus* injected into the tibial marrow cavity), model + vehicle group (model rabbits treated with normal saline for 4 weeks), and model + CGA group (model rabbits treated with CGA for 4 weeks). (A–C) The proliferation of CD4$^+$ or CD8$^+$ T lymphocytes was determined by flow cytometry. (D) IL-2 levels in peripheral blood were measured by ELISA. (E) The expression of IL-2 in peripheral blood was quantified by qRT-PCR, using Gapdh as an internal control. All assays were performed in triplicate and/or repeated in at least three independent experiments. ***$p < 0.001$.

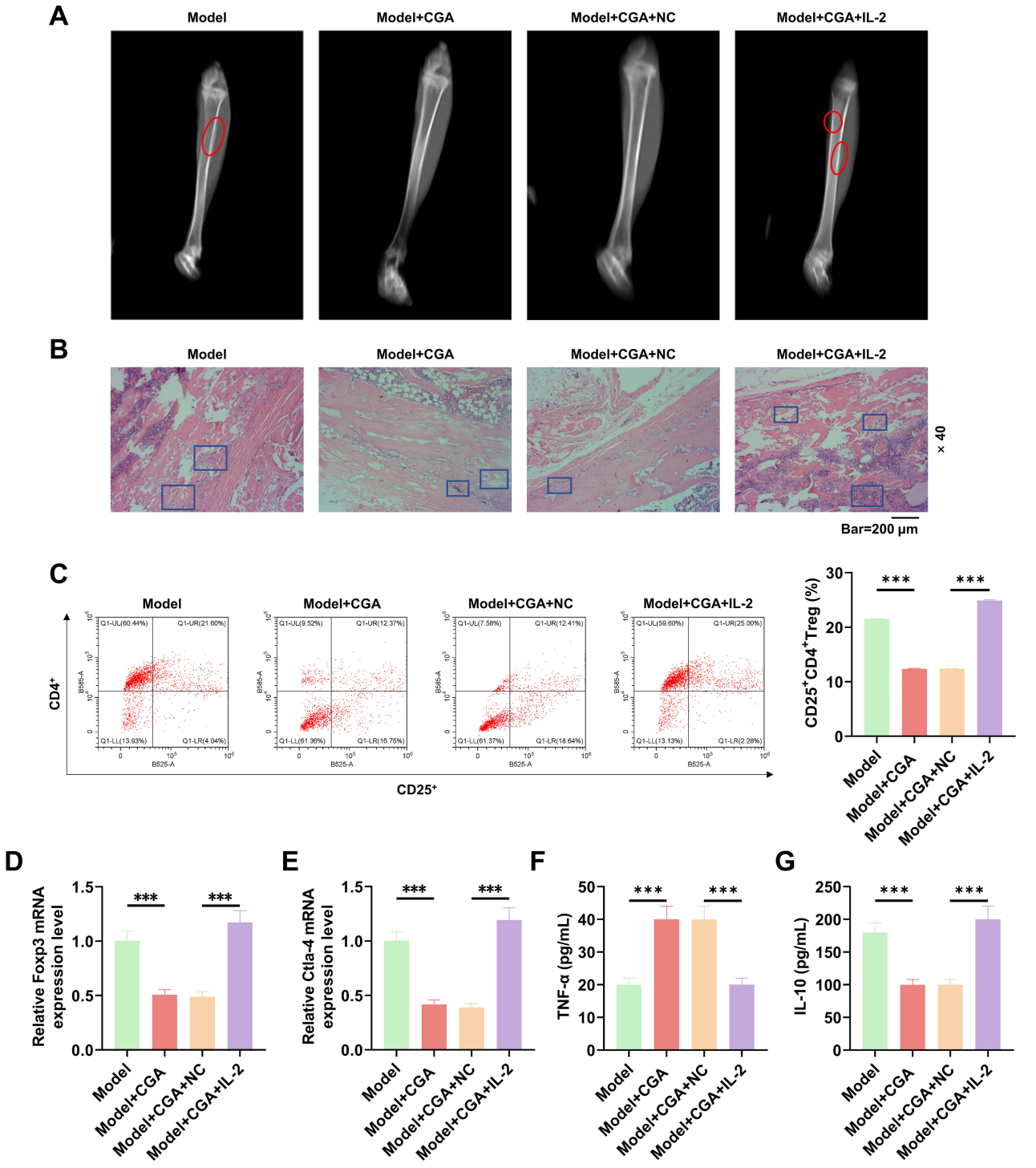

Fig. 4. IL-2 reversed the therapeutic effect of CGA in a rabbit model of PTO. New Zealand white rabbits were assigned to four groups (n = 5/each group): model group (*Staphylococcus aureus* injected into the tibial marrow cavity), model + CGA group (model rabbits treated with CGA for 4 weeks), model + CGA + negative control (NC) group (model rabbits treated with CGA and injected with lentiviral negative control) and model + CGA + IL-2 group (model rabbits treated with CGA and injected with lentivirus expressing IL-2 through the tail vein 24 h before receiving treatment). (A) Micro-CT images showing tibial defects (red circles indicate hyperosteogeny and inflammation). (B) Histological alterations were evaluated by HE staining (40× magnification, scale bar = 200 μm); blue boxes indicate osteoporosis, severe cortical bone destruction, fibrous tissue hyperplasia, and inflammatory cell infiltration. (C) The proportion of $CD25^{+}CD4^{+}$ Treg was detected by flow cytometry. (D,E) *Foxp3* and *Ctla-4* expression levels were determined by qRT-PCR, with *Gapdh* as an internal control. (F,G) TNF-α and IL-10 concentrations in peripheral blood were measured by ELISA. All assays were performed in triplicate and/or repeated in at least three independent experiments. ***$p < 0.001$.

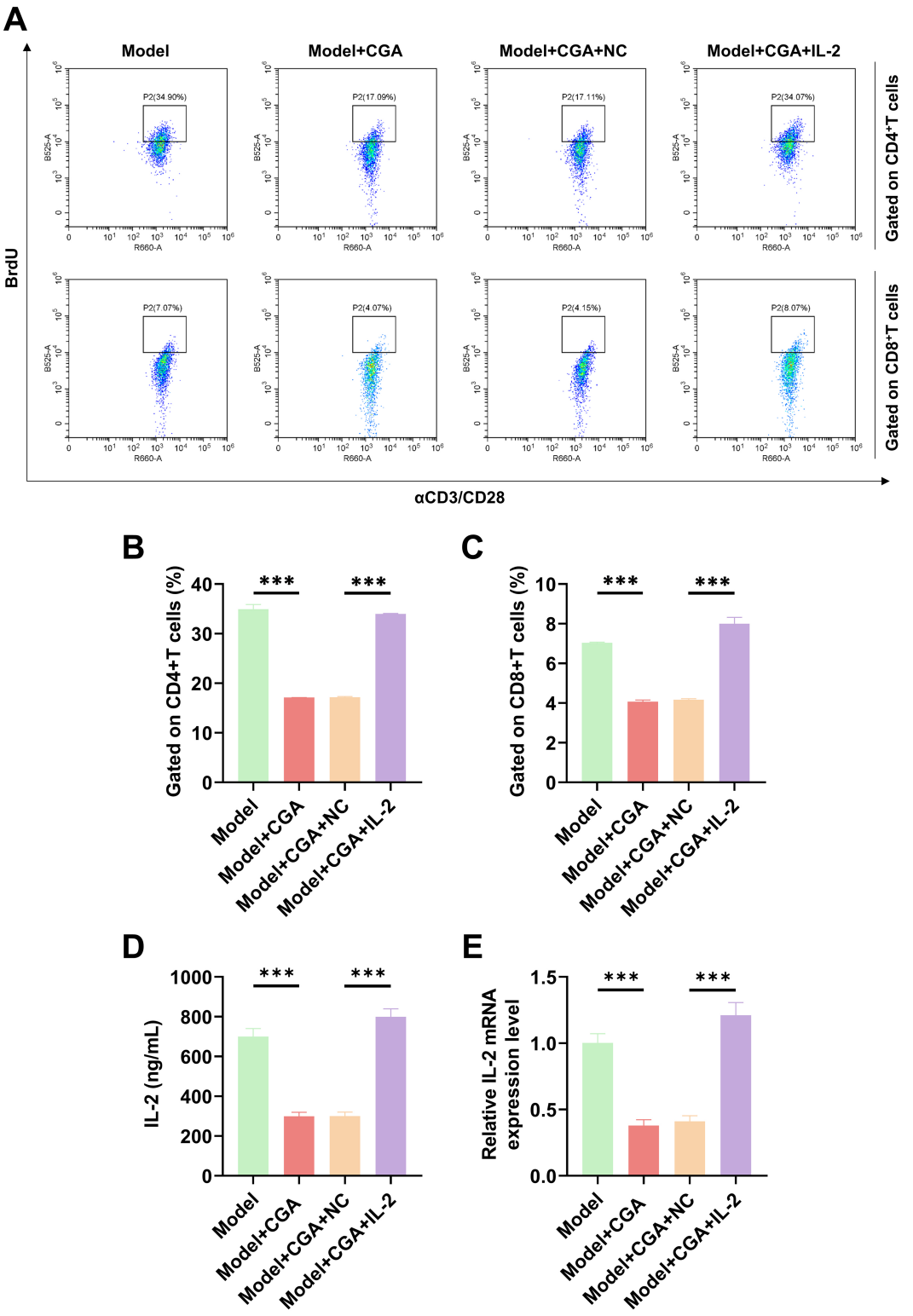

Fig. 5. IL-2 reversed the effects of CGA on CD4$^+$ and CD8$^+$ T lymphocyte proliferation and expression in PTO rabbits. New Zealand white rabbits were distributed into four groups (n = 5/each group): model group (*Staphylococcus aureus* injected into the tibial marrow cavity), model + CGA group (model rabbits treated with CGA for 4 weeks), model + CGA + NC group (model rabbits treated with CGA and injected with lentiviral negative control), and model + CGA + IL-2 group (model rabbits injected with lentivirus expressing IL-2 through the tail vein 24 h before *S. aureus* injection, followed by daily administration of CGA by gavage for 4 weeks). (A–C) Proliferation of CD4$^+$ or CD8$^+$ T lymphocytes was determined by flow cytometry. (D) The concentration of IL-2 in peripheral blood was quantified by ELISA. (E) The expression of *IL-2* in peripheral blood was measured by qRT-PCR, with *Gapdh* as an internal control. All assays were performed in triplicate and/or repeated in at least three independent experiments. ***$p < 0.001$.

Tregs are derived from $CD4^+$ T cells, while $CD4^+$ T cells can impair bone quality and cause bone fragility [32], and $CD8^+$ T cells can induce bone erosion [33]. These findings highlight the complex and dual role of $CD4^+$/$CD8^+$ T cells in PTO pathology.

Notably, long-term dysregulation of Tregs may impede osteomyelitis recovery. Qi-Fen Mao *et al*. [34] reported that excessive immunosuppression due to upregulated Treg levels in osteomyelitis could lead to persistent infectious inflammation, necessitating immunomodulatory drug interventions. CGA, a natural phenolic compound abundantly present in coffee and various plants, exhibits multiple biological activities, including antioxidant, anti-inflammatory, and immunomodulatory effects. The previous study has demonstrated that CGA effectively promotes T cell infiltration in tumors [13]. Additionally, a caffeic acid (CHA)-phospholipid complex (PC)-containing polyethylene glycol (PEG)-modified liposomes formulation has been reported to stimulate $CD4^+$ and $CD8^+$ T cell infiltration, enhance memory T cell populations, and inhibit infiltration of myeloid-derived suppressor cells [35]. In our study, CGA improved PTO symptoms, lowered Tregs proportion, and inhibited the proliferation of $CD4^+$/$CD8^+$ T cells. The improvement in PTO symptoms observed with CGA treatment may be partly attributed to Treg inhibition. Interestingly, the therapeutic effect of CGA in PTO was reversed by IL-2 administration. Therefore, CGA may weaken the function of Treg by inhibiting IL-2 expression, thus improving PTO symptoms. However, the precise signaling pathways through which CGA modulates the biological behavior of PTO remain unclear and warrant further investigation. Moreover, CGA has been reported to reduce the ratio of $CD4^+$IL-17^+ Th17 cells to $CD4^+$ T cells in peripheral blood [36]. These findings suggest that Th17 cells may also be involved in the mechanism by which CGA alleviates PTO, highlighting the need for further investigations to explore this potential pathway.

In addition, PTO remains a significant challenge in the field of trauma treatment. Rabbits are commonly used to replicate trauma and surgical interventions due to their ease of handling, relatively low breeding costs, and well-established surgical techniques. However, their immune response to infection differs from that of humans, and their bone structure does not replicate human bone as closely as that of rats or mice. Therefore, the continuous development of new technologies is needed to provide more diverse and innovative treatment options for PTO. Multidisciplinary research approaches and personalized treatment strategies are emerging as important future research directions.

This study has several limitations. First, although we demonstrated that CGA exerts its therapeutic effects through the modulation of IL-2, the exact mechanism of action remains to be further explored. Second, the study primarily focused on the short-term efficacy of CGA, while its long-term safety and sustained effectiveness remain to be determined. Furthermore, the absence of a sham control group limits the ability to confirm that our findings are specific to *Staphylococcus aureus*-induced PTO.

Conclusion

In summary, our study demonstrates the therapeutic effect of CGA in a PTO animal model and reveals that its mechanism of action is associated with the inhibition of IL-2-mediated enhancement of Treg function. These findings provide a theoretical foundation for the potential application of CGA in the treatment of PTO.

Availability of Data and Materials

The analyzed data sets generated during the study are available from the corresponding author on reasonable request.

Author Contributions

YL designed the research study; ZW and YN performed the research; YZ, LL and SY collected and analyzed the data. All authors have been involved in drafting the manuscript and all authors have been involved in revising it critically for important intellectual content. All authors approve the final version to be published. All authors have participated sufficiently in the work to take public responsibility for appropriate portions of the content and agreed to be accountable for all aspects of the work in ensuring that questions related to its accuracy or integrity.

Ethics Approval and Consent to Participate

According to the guidelines of the China Council on Animal Care and Use, all experiments in this study were approved by the Laboratory Animal Ethics Committee of Hangzhou Normal University (Approval No. 2023041).

Acknowledgment

Not applicable.

Funding

This work was supported by the Zhejiang Province Traditional Chinese Medicine Science and Technology Project [No. 2023ZL614].

Conflict of Interest

The authors declare no conflict of interest.

Supplementary Material

Supplementary material associated with this article can be found, in the online version, at https://doi.org/10.24976/Discov.Med.202537197.90.

References

[1] Ren Y, Liu L, Sun D, Zhang Z, Li M, Lan X, *et al*. Epidemiological updates of post-traumatic related limb osteomyelitis in China: a 10 years multicentre cohort study. International Journal of Surgery (London, England). 2023; 109: 2721–2731. https://doi.org/10.1097/JS9.0000000000000502.

[2] Tang B, Zhu W. Progress in diagnosis and treatment of post-traumatic osteomyelitis. Zhong Nan Da Xue Xue Bao. Yi Xue Ban = Journal of Central South University. Medical Sciences. 2021; 46: 1290–1297. https://doi.org/10.11817/j.issn.1672-7347.2021.200621.

[3] Yang J, Yao JL, Wu ZQ, Zeng DL, Zheng LY, Chen D, *et al*. Current opinions on the mechanism, classification, imaging diagnosis and treatment of post-traumatic osteomyelitis. Chinese Journal of Traumatology = Zhonghua Chuang Shang Za Zhi. 2021; 24: 320–327. https://doi.org/10.1016/j.cjtee.2021.07.006.

[4] Böhm E, Josten C. What's new in exogenous osteomyelitis? Pathology, Research and Practice. 1992; 188: 254–258. https://doi.org/10.1016/S0344-0338(11)81195-7.

[5] Deng Z, Zhang Q, Zhao Z, Li Y, Chen X, Lin Z, *et al*. Crosstalk between immune cells and bone cells or chondrocytes. International Immunopharmacology. 2021; 101: 108179. https://doi.org/10.1016/j.intimp.2021.108179.

[6] Wu Y, Tang Y, Liang X, Lin Y, Yang W, Ma Y, *et al*. The role of increased frequency of treg cells in patients with chronic osteomyelitis. Orthopedics. 2011; 34: 98. https://doi.org/10.3928/01477447-20101221-16.

[7] Kwack KH, Lee HW. Progranulin Inhibits Human T Lymphocyte Proliferation by Inducing the Formation of Regulatory T Lymphocytes. Mediators of Inflammation. 2017; 2017: 7682083. https://doi.org/10.1155/2017/7682083.

[8] Rojas-González A, Figueroa-Hernández CY, González-Rios O, Suárez-Quiroz ML, González-Amaro RM, Hernández-Estrada ZJ, *et al*. Coffee Chlorogenic Acids Incorporation for Bioactivity Enhancement of Foods: A Review. Molecules (Basel, Switzerland). 2022; 27: 3400. https://doi.org/10.3390/molecules27113400.

[9] Girsang E, Ginting CN, Lister INE, Gunawan KY, Widowati W. Anti-inflammatory and antiaging properties of chlorogenic acid on UV-induced fibroblast cell. PeerJ. 2021; 9: e11419. https://doi.org/10.7717/peerj.11419.

[10] Tan H, Zhen W, Bai D, Liu K, He X, Ito K, *et al*. Effects of dietary chlorogenic acid on intestinal barrier function and the inflammatory response in broilers during lipopolysaccharide-induced immune stress. Poultry Science. 2023; 102: 102623. https://doi.org/10.1016/j.psj.2023.102623.

[11] Xue W, Hao J, Zhang Q, Jin R, Luo Z, Yang X, *et al*. Chlorogenic Acid Inhibits Epithelial-Mesenchymal Transition and Invasion of Breast Cancer by Down-Regulating LRP6. The Journal of Pharmacology and Experimental Therapeutics. 2023; 384: 254–264. https://doi.org/10.1124/jpet.122.001189.

[12] Zhu H, Shen F, Wang X, Qian H, Liu Y. Chlorogenic acid improves the cognitive deficits of sleep-deprived mice via regulation of immunity function and intestinal flora. Phytomedicine: International Journal of Phytotherapy and Phytopharmacology. 2024; 123: 155194. https://doi.org/10.1016/j.phymed.2023.155194.

[13] Li R, Zhan Y, Ding X, Cui J, Han Y, Zhang J, *et al*. Cancer Differentiation Inducer Chlorogenic Acid Suppresses PD-L1 Expression and Boosts Antitumor Immunity of PD-1 Antibody. International Journal of Biological Sciences. 2024; 20: 61–77. https://doi.org/10.7150/ijbs.83599.

[14] Li S, Wang H, Wu H, Chang X. Therapeutic Effect of Exogenous Regulatory T Cells on Collagen-induced Arthritis and Rheumatoid Arthritis. Cell Transplantation. 2020; 29: 963689720954134. https://doi.org/10.1177/0963689720954134.

[15] Li Y, Chen L, Lin M, Wang C, Zhang R, Li Y, *et al*. Micro-CT analysis of osteomyelitis of rabbit tibial for model establishment and biomaterials application in tissue engineering. Heliyon. 2022; 8: e12471. https://doi.org/10.1016/j.heliyon.2022.e12471.

[16] Worlock P, Slack R, Harvey L, Mawhinney R. An experimental model of post-traumatic osteomyelitis in rabbits. British Journal of Experimental Pathology. 1988; 69: 235–244.

[17] Ji R, Chen J, Xu J, Zhang L, Liu L, Li F. Protective effect of chlorogenic acid on liver injury in heat-stressed meat rabbits. Journal of Animal Physiology and Animal Nutrition. 2024; 108: 1203–1213. https://doi.org/10.1111/jpn.13966.

[18] Chen J, Song Z, Ji R, Liu Y, Zhao H, Liu L, *et al*. Chlorogenic acid improves growth performance of weaned rabbits *via* modulating the intestinal epithelium functions and intestinal microbiota. Frontiers in Microbiology. 2022; 13: 1027101. https://doi.org/10.3389/fmicb.2022.1027101.

[19] Chen X, Jiao J, He X, Zhang J, Wang H, Xu Y, *et al*. CHI3L1 regulation of inflammation and the effects on osteogenesis in a Staphylococcus aureus-induced murine model of osteomyelitis. The FEBS Journal. 2017; 284: 1738–1747. https://doi.org/10.1111/febs.14082.

[20] Sun Y, Hu L, Yang P, Zhang M, Wang X, Xiao H, *et al*. pH Low Insertion Peptide-Modified Programmed Cell Death-Ligand 1 Potently Suppresses T-Cell Activation Under Acidic Condition. Frontiers in Immunology. 2021; 12: 794226. https://doi.org/10.3389/fimmu.2021.794226.

[21] Harris F, Berdugo YA, Tree T. IL-2-based approaches to Treg enhancement. Clinical and Experimental Immunology. 2023; 211: 149–163. https://doi.org/10.1093/cei/uxac105.

[22] Borlongan MC, Kingsbury C, Salazar FE, Toledo ARL, Monroy GR, Sadanandan N, *et al*. IL-2/IL-2R Antibody Complex Enhances Treg-Induced Neuroprotection by Dampening TNF-α Inflammation in an In Vitro Stroke Model. Neuromolecular Medicine. 2021; 23: 540–548. https://doi.org/10.1007/s12017-021-08656-0.

[23] Jung MK, Lee JS, Kwak JE, Shin EC. Tumor Necrosis Factor and Regulatory T Cells. Yonsei Medical Journal. 2019; 60: 126–131. https://doi.org/10.3349/ymj.2019.60.2.126.

[24] Guarch-Pérez C, Riool M, Zaat SA. Current osteomyelitis mouse models, a systematic review. European Cells & Materials. 2021; 42: 334–374. https://doi.org/10.22203/eCM.v042a22.

[25] Xiao L, Li T, Ding M, Yang J, Rodríguez-Corrales J, LaConte SM, *et al*. Detecting Chronic Post-Traumatic Osteomyelitis of Mouse Tibia via an IL-13Rα2 Targeted Metallofullerene Magnetic Resonance Imaging Probe. Bioconjugate Chemistry. 2017; 28: 649–658. https://doi.org/10.1021/acs.bioconjchem.6b00708.

[26] Arens D, Wilke M, Calabro L, Hackl S, Zeiter S, Zderic I, *et al*. A rabbit humerus model of plating and nailing osteosynthesis with and without Staphylococcus aureus osteomyelitis. European Cells & Materials. 2015; 30: 148–161; discussion 161–162. https://doi.org/10.22203/ecm.v030a11.

[27] Malviya V, Yshii L, Junius S, Garg AD, Humblet-Baron S, Schlenner SM. Regulatory T-cell stability and functional plasticity in health and disease. Immunology and Cell Biology. 2023; 101: 112–129. https://doi.org/10.1111/imcb.12613.

[28] McCallion O, Bilici M, Hester J, Issa F. Regulatory T-cell therapy approaches. Clinical and Experimental Immunology. 2023; 211: 96–107. https://doi.org/10.1093/cei/uxac078.

[29] Wagner C, Heck D, Lautenschläger K, Iking-Konert C, Heppert V, Wentzensen A, *et al*. T lymphocytes in implant-associated posttraumatic osteomyelitis: Identification of cytotoxic T effector cells at the site of infection. Shock (Au-

gusta, Ga.). 2006; 25: 241–246. https://doi.org/10.1097/01.shk.0000192119.68295.14.

[30] Friot A, Djebali S, Valsesia S, Parroche P, Dubois M, Baude J, *et al*. Antigen specific activation of cytotoxic $CD8^+$ T cells by *Staphylococcus aureus* infected dendritic cells. Frontiers in Cellular and Infection Microbiology. 2023; 13: 1245299. https://doi.org/10.3389/fcimb.2023.1245299.

[31] Wik JA, Skålhegg BS. T Cell Metabolism in Infection. Frontiers in Immunology. 2022; 13: 840610. https://doi.org/10.3389/fimmu.2022.840610.

[32] Cifuentes-Mendiola SE, Solis-Suarez DL, Martínez-Dávalos A, Godínez-Victoria M, García-Hernández AL. $CD4^+$ T-cell activation of bone marrow causes bone fragility and insulin resistance in type 2 diabetes. Bone. 2022; 155: 116292. https://doi.org/10.1016/j.bone.2021.116292.

[33] Joo YB, Park Y, Kim K, Bang SY, Bae SC, Lee HS. Association of $CD8^+$ T-cells with bone erosion in patients with rheumatoid arthritis. International Journal of Rheumatic Diseases. 2018; 21: 440–446. https://doi.org/10.1111/1756-185X.13090.

[34] Mao QF, Shang-Guan ZF, Chen HL, Huang K. Immunoregulatory role of IL-2/STAT5/CD4+CD25+Foxp3 Treg pathway in the pathogenesis of chronic osteomyelitis. Annals of Translational Medicine. 2019; 7: 384. https://doi.org/10.21037/atm.2019.07.45.

[35] Zhang Y, Yang Y, Ye J, Gao Y, Liao H, Zhou J, *et al*. Construction of chlorogenic acid-containing liposomes with prolonged antitumor immunity based on T cell regulation. Science China. Life Sciences. 2021; 64: 1097–1115. https://doi.org/10.1007/s11427-020-1739-6.

[36] Shi Z, Jiang W, Chen X, Xu M, Wang J, Lai Y, *et al*. Chlorogenic acid ameliorated allergic rhinitis-related symptoms in mice by regulating Th17 cells. Bioscience Reports. 2020; 40: BSR20201643. https://doi.org/10.1042/BSR20201643.